

# Frustrated spin-1/2 ladder with ferro- and antiferromagnetic legs

Debasmita Maiti, Dayasindhu Dey, Manoranjan Kumar\*

*S. N. Bose National Centre for Basic Sciences, Block JD, Sector III, Salt Lake, Kolkata - 700106, India*

---

## Abstract

Two-leg spin-1/2 ladder systems consisting of a ferromagnetic leg and an antiferromagnetic leg are considered where the spins on the legs interact through antiferromagnetic rung couplings  $J_1$ . These ladders can have two geometrical arrangements either zigzag or normal ladder and these systems are frustrated irrespective of their geometry. This frustration gives rise to incommensurate spin density wave, dimer and spin fluid phases in the ground state. The magnetization in the systems decreases linearly with  $J_1^2$ , and the systems show an incommensurate phase for  $0.0 < J_1 < 1.0$ . The spin-spin correlation functions in the incommensurate phase follow power law decay which is very similar to Heisenberg antiferromagnetic chain in external magnetic field. In large  $J_1$  limit, the normal ladder behaves like a collection of singlet dimers, whereas the zigzag ladder behaves as a one dimensional spin-1/2 antiferromagnetic chain.

*Keywords:* Frustrated magnetic systems, incommensurate phase, dimer phase, bilayer magnetic materials

---

## 1. Introduction

The theoretical studies of magnetic spin-1/2 ladder systems have been an active area of research because of the existence of interesting phases like dimer [1], spiral phase [2], different ordered phases [3], magnetization plateau [4] etc. The spin-1/2 ladder model systems show a rich quantum phase diagrams in various interaction coupling limit. The Heisenberg antiferromagnetic (HAF) spin-1/2 normal ladder is realized in  $\text{SrCu}_2\text{O}_3$  [5],  $(\text{VO})_2\text{P}_2\text{O}_7$  etc. [6, 7], whereas zigzag ladder, which is considered as the chain with nearest and next nearest neighbor interactions, have been realized in  $(\text{N}_2\text{H}_5)\text{CuCl}_3$  [8],  $\text{LiCuSbO}_4$  [9],  $\text{LiSbVO}_4$  [10],  $\text{Li}_2\text{CuZrO}_4$  [11] etc. The AF normal ladder system is a spin liquid with a spin gap and short range spin correlation. It was conjectured that the spin gap decreases smoothly as rung exchange interaction decreases [1, 12, 13] and reduces to zero only when rung interaction strength approaches to zero. The rung interaction induces the singlet dimer formation between the two nearest spin-1/2 on different legs [7,

---

\*Corresponding author

Email address: manoranjan.kumar@bose.res.in (Manoranjan Kumar)

Preprint submitted to Elsevier

October 5, 2018

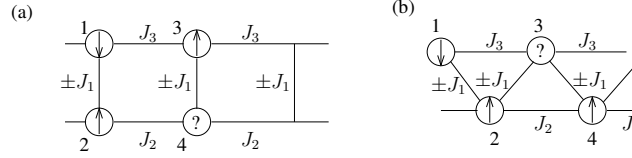


Figure 1: (a) and (b) show the normal and the zigzag arrangements of the interfaces. The arrows show the spin arrangement and the question mark represents the frustrated spin.

[12]. Ladders with ferromagnetic legs/rungs and antiferromagnetic rungs/legs are also well studied and show interesting phases [14–19]. However, the AF zigzag ladder is completely different from normal ladder. The zigzag ladder in the weak rung coupling limit  $J_1/J_2 < 0.44$  behaves like two independent HAF spin-1/2 chains [2, 20, 21], and shows gapped spiral phase for  $0.44 < J_1 < 2$ . It is gapped system with dimer configuration for  $2 < J_1/J_2 < 4.148$  [2, 20–23].

In this paper we consider spin ladders which have ferromagnetic (F) spin exchange interactions along one of the legs, and antiferromagnetic (AF) interactions on the other leg; and spins on these two legs are interacting through AF interaction. The focus of this paper is to study some universal theoretical aspects such as the existence of exotic phases in the ground state (GS) and low-lying excitations in this system. We show that the ferromagnetic-antiferromagnetic (F-AF) ladders pose quasi-long range behavior in incommensurate regime, and frustration can be induced even for very small rung coupling limit.

These two lagged ladders can represent the interface of the two layered magnetic spin-1/2 system consisting of an antiferromagnetic and a ferromagnetic layer where the two layers interact with direct or indirect antiferromagnetic exchange. Similar interfaces are studied by Suhl *et al.* [24] and Hong *et al.* [25]. We further simplify the model by considering only a inter-facial line of spins in the interface of both the layers. We consider two possibilities of arrangement of inter-facial spins; first, when spins are directly facing each-other as in normal ladder (NL), and second, where spins on one leg is shifted by half of the lattice unit forming a zigzag ladder (ZL). The spin arrangements of NL and ZL are shown in the Fig. 1(a) and (b). These systems are interesting because both the ladders are frustrated irrespective to the nature of rung interactions.

These spin-1/2 NL or ZL can also give some preliminary information about the phases at the interface of bilayer F-AF magnetic thin films. The inter-facial properties of the F-AF thin film materials [26, 27] remain a subject of active research till date. At low temperature (below Néel temperature and Curie temperature), the spins on both the layers remain ordered. This leads to an exchange bias at the interface. Many theoretical models based on microstructure have been proposed to explain the exchange bias field phenomenon [26–30] at the interface of these F-AF layers, e.g., discrete micromagnetics models [31–38], continuum micromagnetics models [39–41], and many others [24, 42, 43]. Suhl [24] considered only the interfacial spins similar to our model and pointed out, the spins at the antiferromagnetic side of the interface is in the mean field of the ferromagnetic spins. This happens because the Néel temperature is lower than the Curie temperature, and the spins on the ferromagnetic side is more robust.

This paper is divided into four sections. In Section 2, the model Hamiltonian is

introduced and the numerical methods are explained. The numerical results for both the ladders are given in Section 3 and the effective model Hamiltonian is constructed in Section 4. All the results are discussed and summarized in Section 5.

## 2. Model Hamiltonian and Numerical Method

We consider a 2-leg ladder (either NL or ZL) of F and AF legs. We further consider the half-filled insulating case where the electrons are completely localized, but spins can interact with its nearest neighbors. Thus we can write an isotropic Heisenberg spin-1/2 model Hamiltonian for the system shown in Figs. 1 (a) and (b) as

$$H = H_{\text{rung}} + H_{\text{leg}}, \quad (1)$$

where

$$\begin{aligned} H_{\text{leg}} &= \sum_{i=1}^{N/2-1} J_2 \vec{S}_{2i} \cdot \vec{S}_{2i+2} + J_3 \vec{S}_{2i-1} \cdot \vec{S}_{2i+1}, \\ H_{\text{rung}}^{\text{NL}} &= J_1 \sum_{i=1}^{N/2} \vec{S}_{2i-1} \cdot \vec{S}_{2i}, \\ H_{\text{rung}}^{\text{ZL}} &= J_1 \sum_{i=1}^{N-1} \vec{S}_i \cdot \vec{S}_{i+1}. \end{aligned} \quad (2)$$

Here the rung Hamiltonian for the NL and ZL are written as  $H_{\text{rung}}^{\text{NL}}$  and  $H_{\text{rung}}^{\text{ZL}}$ , respectively. The nearest neighbor AF interaction  $J_3$  is along the upper leg, and nearest neighbor F interaction  $J_2$  is along the lower leg.  $J_1$  is interaction along the rung of the systems as shown in Fig. 1(a) and Fig. 1(b) for the NL and the ZL, respectively. The interactions along legs are set to  $J_2 = -1$  and  $J_3 = 1$ , however, rung interaction ( $J_1 = \alpha$ ) is a variable quantity. To understand the GS properties of these systems as a function of  $\alpha$ , we solve the Hamiltonian in Eq. (1) numerically.

We use the exact diagonalization (ED) method for small systems and Density matrix renormalization group (DMRG) method to handle the large degrees of freedom for large systems. The DMRG is based on the systematic truncation of irrelevant degrees of freedom at every step of growth of the chain [44–46]. We have used recently developed DMRG method where four new sites are added at every DMRG steps [47]. We have also used the recently developed DMRG for periodic boundary condition (PBC) when the system is under PBC [48]. The eigenvectors corresponding to  $m$  largest eigenvalues of the density matrix of the system in the GS of Hamiltonian in Eq. (1) are kept to construct the effective density matrix. We have kept  $m$  up to 500 to keep the truncation error less than  $10^{-10}$ . We have used system sizes up to  $N = 200$  to minimize the finite size effect.

## 3. Numerical Results

In this section, we analyze the GS of both the ZL and the NL for various rung interaction ( $\alpha$ ) limits. Here we consider only the antiferromagnetic inter-chain interaction

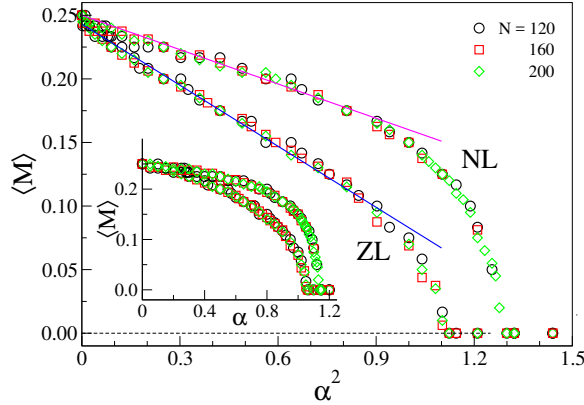


Figure 2: The ground state magnetization  $\langle M \rangle$  with inter chain coupling interaction  $\alpha$  for both the NL and the ZL. The main figure plots  $\langle M \rangle$  vs.  $\alpha^2$ ; the straight line fits for  $\alpha < 0.9$  i.e.,  $\alpha^2 < 0.8$  reveals that  $\langle M \rangle \propto \alpha^2$  in this regime. The inset shows the  $\langle M \rangle - \alpha$  curve.

i.e.,  $\alpha > 0$ . In the small  $\alpha (\ll 1)$  limit, the NL and the ZL behave like decoupled chains. In this phase the F leg remains in ferromagnetic state, whereas other leg possesses antiferromagnetic arrangement of spins. However, in thermodynamic limit the decoupled phase exists only for  $\alpha \sim 0$ . On further increase in  $\alpha$ , the competition between the F and the AF interactions forces the F leg to reduce its total magnetization. There is an incommensurate spin density wave (SDW) phase for parameter space  $0.07 < \alpha < 1.14$  in the NL and  $0.04 < \alpha < 1.06$  for the ZL with  $N = 200$  spins. In thermodynamic limit, the lower limit of  $\alpha$  value for SDW phase tends to zero. In the large  $\alpha$  limit of the NL, the two nearest neighbor spins from different legs form a singlet dimer. However, the ZL behaves like a single spin-1/2 chain of  $N$  spins where each leg contains  $N/2$  spins. To verify the above phases, total magnetization  $\langle M \rangle$  in GS, correlation functions  $C(r)$ , and the spin densities  $\rho_r$  for both the systems are analyzed.

### 3.1. Magnetization

For small inter-chain antiferromagnetic coupling ( $\alpha \ll 1$ ), two legs of the ladder behave as decoupled chains, and the system has its ground state magnetization  $\langle M \rangle = \frac{\sum_{i=1}^N S_i^z}{N} = \frac{1}{4}$ . All of the magnetization contribution comes from the F leg. The magnetization  $\langle M \rangle$  decreases continuously with  $\alpha$ , and  $\langle M \rangle$  goes finally to zero for large  $\alpha$ . The  $\langle M \rangle$  as a function of  $\alpha^2$  is shown in Fig. 2 (main) for three system sizes  $N = 120, 160$ , and 200 of both the NL and the ZL systems, and the inset show the  $\langle M \rangle - \alpha$  curve. We notice there are step like behavior in  $\langle M \rangle - \alpha$  plot in finite system, but width of steps decreases with system size  $N$ . However,  $\langle M \rangle - \alpha$  curve should be continuous in the thermodynamic limit. We notice that the NL shows slower change in  $\langle M \rangle - \alpha$  as compared to the ZL.

The transition from incommensurate SDW phase to spin fluid phase at  $\alpha = \alpha_c = 1.06$  is relatively faster in the ZL compared to the transition from incommensurate SDW to dimer phase at  $\alpha = \alpha_c = 1.14$  in the NL, and the  $\langle M \rangle$  vanishes at the transition point  $\alpha = \alpha_c$ . In fact our analytical perturbation calculation for the NL in Sec. 4 also suggests that the contribution from interaction along the legs are zero at large  $\alpha$  limit. In this limit

the NL system of  $N$  spins behaves as a collection of  $\frac{N}{2}$  number of independent singlet dimers. The continuous variation in the ZL near the transition point can be attributed to delocalized nature of the system. In this limit  $J_1$  dominates, and this system behaves like a HAF spin-1/2 chain with weak and alternate AF and F next nearest neighbor interaction. The ferromagnetic interaction  $J_2$  stabilize the AF arrangement of spins, whereas AF interaction  $J_3$  frustrates the system.

To understand the spin arrangement and correlation between the spins, spin correlations and spin densities are studied.

### 3.2. Spin-spin correlations

Longitudinal spin-spin correlations are defined as

$$C(r) = \langle S_i^z S_{i+r}^z \rangle \quad (3)$$

where  $S_i^z$  and  $S_{i+r}^z$  are the z-component of spin operators at reference site  $i$  and at a distance  $r$  from the reference site  $i$ , respectively. Our reference site is at the AF leg in this subsection. We have also defined spin density fluctuation as

$$C^F(r) = \langle S_i^z S_{i+r}^z \rangle - \langle S_i^z \rangle \langle S_{i+r}^z \rangle. \quad (4)$$

We find three types of correlations for both the ladder systems in different parameter regimes as shown in Fig. 3. Black circles represent correlations with spins located on AF leg, whereas squares represent the correlations with the spins on F leg.  $C(r)$  for three different phases are shown in Figs. 3(a)–(c) for the NL and Figs. 3(d)–(f) for the ZL with  $N=200$ . For  $\alpha = 0.05$ , the spins on different legs are uncorrelated, and the spins on the AF leg show quasi-long-range order, as shown in Fig. 3(a). The similar behavior is found in the ZL for  $\alpha = 0.01$  as shown in Fig. 3(d). The incommensurate phase in the NL is observed for  $0.07 < \alpha < 1.14$  and in the ZL for  $0.04 < \alpha < 1.06$ . We choose  $\alpha = 0.45$  for the NL and  $\alpha = 0.25$  for the ZL to make sure that we have same  $S^z$  value in both types of ladder. At large distance  $r$ , the value of  $C(r)$  for both the NL and the ZL is finite as shown in Fig. 3(b) for NL and Fig. 3(e) for ZL. However,  $C^F(r)$  decays algebraically for the AF and the F leg separately where we consider the reference spin on the AF and the F leg, respectively.

At large  $\alpha$  limit ( $\alpha \geq 1.16$ ), the behavior of the two ladders become completely different. In NL the  $C(r)$  have non-zero value only up to  $r = 1$ , as shown in Fig. 3(c). In the large  $\alpha$  ( $\geq 1.06$ ) limit the ZL behaves like a single antiferromagnetic Heisenberg chain and the  $C(r)$  decays following a power law ( $\propto r^{-\gamma}$ ) where spins from AF and F leg situated alternatively with distance  $r$ . The  $C(r)$  in this regime is shown in Fig. 3(f) for  $\alpha = 1.06$ .

The incommensurate SDW phases for the NL and the ZL are similar to that in the HAF spin-1/2 chain in a magnetic field; therefore,  $C(r)$  in the F and the AF legs are analyzed separately for both the NL and the ZL.  $C^F(r)$  for the F leg in both the systems are vanishingly small. To understand it better, we plot  $C^F(r)$  for the AF leg in Figs. 4(a) and (b) for the NL and the ZL, respectively, for same  $\alpha$  ( $= 0.2$ ) and  $N = 200$ . We find that  $C^F(r)$  in AF leg for both the systems follow the relation

$$C^F(r) \propto (-1)^r r^{-\gamma} \sin\left(\frac{\pi(r+c)}{\beta}\right) \quad (5)$$

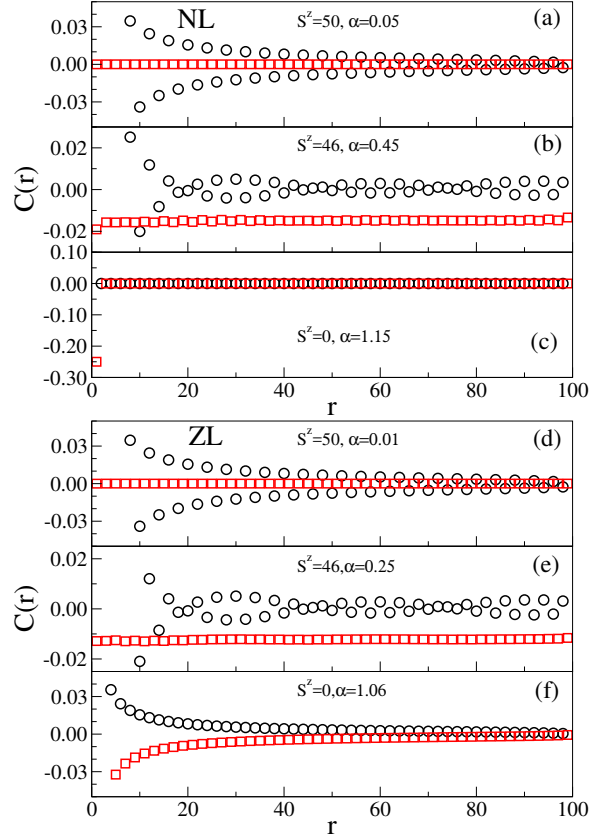


Figure 3: The longitudinal spin-spin correlations  $C(r)$  are plotted for  $N=200$  considering the reference spin on the AF leg. Here circles represent  $C(r)$  with the spins of the AF leg whereas squares represent  $C(r)$  with the spins of the F leg. Different values of  $\alpha$  are chosen to show the (a) decoupled phase, (b) incommensurate SDW phase, (c) dimer phase for  $\alpha = 0.05, 0.45, 1.15$  respectively in the NL, and (d) decoupled phase, (e) incommensurate SDW phase, (f) spin-fluid phase for  $\alpha = 0.01, 0.25, 1.06$  respectively in the ZL.

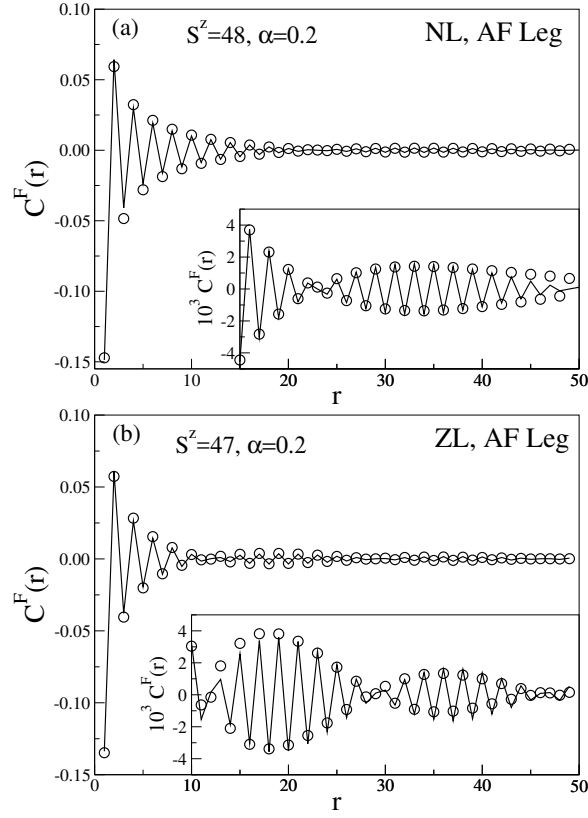


Figure 4: Spin density fluctuations  $C^F(r)$  for the spins on the AF leg for (a) NL and (b) ZL. The reference spin is on the AF leg. The points are the ground state  $C^F(r)$  calculated using DMRG for  $N = 200$ ,  $\alpha = 0.2$  for both the ladders. Calculated  $C^F(r)$  are fitted using Eq. (5) and the solid lines represent the fitted curves. The insets are the zoomed  $C^F(r)$  plot.

Here  $\beta$  is proportional to wavelength of the SDW,  $\gamma$  represents the power law coefficient, and  $\frac{\pi c}{\beta}$  is a phase shift. In Fig. 4(a) and Fig. 4(b) solid lines are the fitted curves where the symbols indicate numerically calculated values of  $C^F(r)$ .  $\beta$  depends on the value of  $\alpha$ . In the main Fig. 4(a),  $C^F(r)$  for  $\alpha = 0.2$  for the NL is shown, and the values are fitted using Eq. (5) with the values  $\beta = 25$  and  $\gamma = 1.5$ . Fig. 4(b) shows the same for the ZL and the fitted parameter values are  $\beta = 17$  and  $\gamma = 1.25$ . The insets of Fig. 4(a) and Fig. 4(b) are the zoomed  $C^F(r)$  and these show that Eq. (5) fits very well even for large distances. The variation of  $\beta$  with  $\alpha$  is discussed in the subsections 3.3 and 3.4. The  $C^F(r)$  on the F leg have values of order of  $10^{-5} - 10^{-6}$ ; therefore, it is difficult to exactly fit the  $C^F(r)$  values on the F leg.

### 3.3. Spin density

The distribution of the spin density on different legs is important, especially in the higher magnetic states. The spin densities on the odd (even) sites correspond to the spin densities on the AF (F) leg. In Figs. 5(a) and (b), the spin densities of alternate sites in the AF leg are shown for the NL and the ZL respectively. For small  $\alpha$ , three  $S^z$  sectors are considered at different  $\alpha$ . The incommensurate spin density ( $\rho_i$ ) for  $S^z = 49, 46$ , and  $41$  for  $\alpha = 0.1, 0.45$ , and  $0.75$  in the AF leg of the NL are shown in Fig. 5(a).  $\rho_i$  for same values of  $S^z$  for  $\alpha = 0.1, 0.25$ , and  $0.45$  in the AF leg of the ZL system are shown in Fig. 5(b). In these systems the incommensurate SDW phase shows the similar behavior for a given  $S^z$  except at the boundary of the system.  $\rho_i$  in the F leg for both the NL and the ZL also show incommensurate SDW as shown in Figs. 5(c) and (d), respectively. However, the incommensurate SDW is more prominent in smaller  $S^z$ .

The edge spin densities of the F leg in the NL is much smaller than the ZL system. The spin density modulation in the F leg is very small for  $\alpha \rightarrow 0$ ; however, the amplitude of the modulations increase with  $\alpha$ . For a given  $S^z$  incommensurate SDW in ZL has smaller amplitude than that in NL, but both have similar  $\beta$ . For large  $\alpha < \alpha_c$ , the periodicity of the AF and the F legs are the same. The total spin density, on each leg of the system,  $\rho_T$  is shown as a function of  $\alpha$  in Fig. 6. The circle and square of same color represent  $\rho_T$  for the AF and the F leg, respectively, however black and red symbols represent the NL and the ZL, respectively. The  $\rho_T$  value in the AF leg is zero in decoupled limit, and it varies linearly with  $\alpha$  with negative slope in both the systems for  $\alpha < 0.9$ . However, for  $\alpha > 0.9$ ,  $\rho_T$  increases rapidly, and goes to zero at the transition point ( $\alpha_c$ ). In the F leg of both systems,  $\rho_T$  decreases monotonically with  $\alpha^2$  for  $\alpha < 0.9$ ;  $\rho_T$  decreases rapidly to zero near the transition point  $\alpha_c = 1.14$  (1.06) for the NL (the ZL).

If we ignore some points near the edges, the spin densities in Fig. 5 can be fitted with the equation which is proportional to  $\sin(\frac{\pi(r+c)}{\beta})$  part in Eq. (5). For the same value of  $\alpha$ ,  $\rho_i$  and  $C^F(r)$  have same  $\beta$  for a particular system. The lowest density amplitudes at the edges is due to the boundary effect. The AF leg has highest density at the edge and induces highest fluctuation in the F leg. The incommensurate SDW has well defined pitch angle.

### 3.4. Pitch angle

We notice that accurate calculation of the pitch angle ( $\theta$ ) from  $C^F(r)$  becomes extremely difficult because of power law nature of  $C^F(r)$ . However,  $\theta$  can be directly calculated from the spin density calculations. Now let us consider the length of the AF



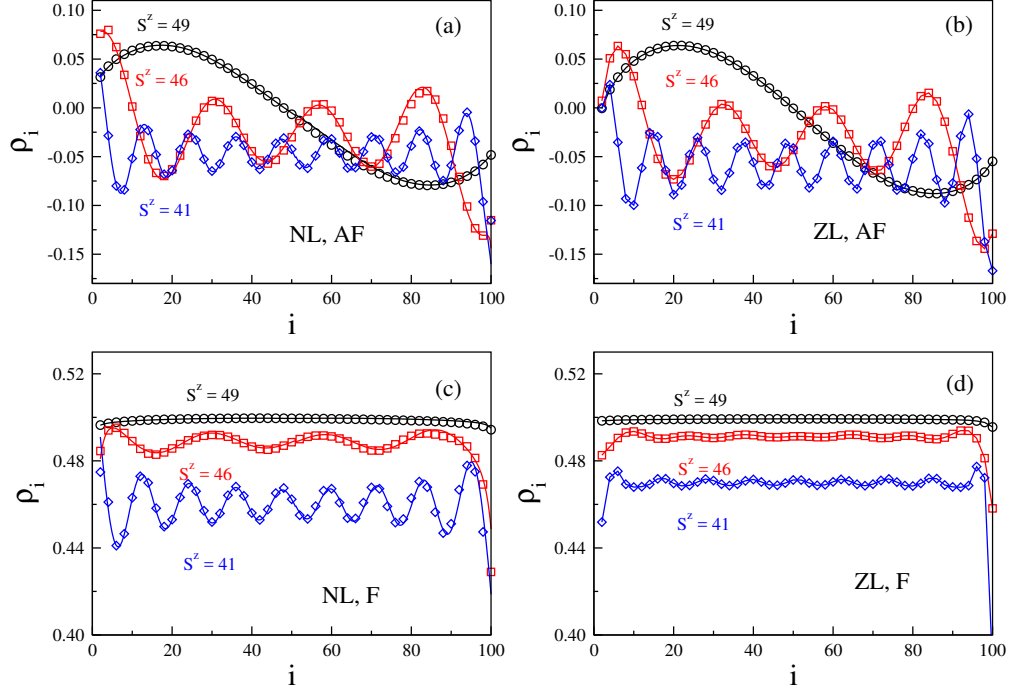


Figure 5: Spin densities for alternate sites on the AF leg and the F leg of the NL and the ZL for  $S^z = 49, 46$  and  $41$ . (a) and (c) depict the spin densities on AF leg and F leg of NL for  $\alpha = 0.1, 0.45, 0.75$  respectively; (b) and (d) show the spin densities on the AF leg and F leg for ZL for  $\alpha = 0.1, 0.25, 0.45$  respectively.

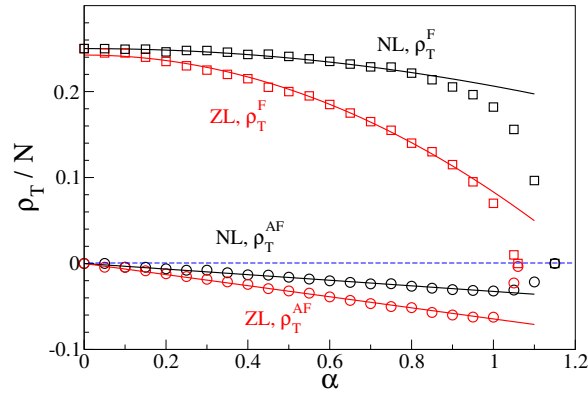


Figure 6: Total spin density on the AF leg and the F leg for both NL and ZL for different values of  $\alpha$ . For  $\alpha < 0.9$  in the F leg  $\rho_T^F \propto \alpha^2$  while in the AF leg  $\rho_T^{AF} \propto \alpha$ .

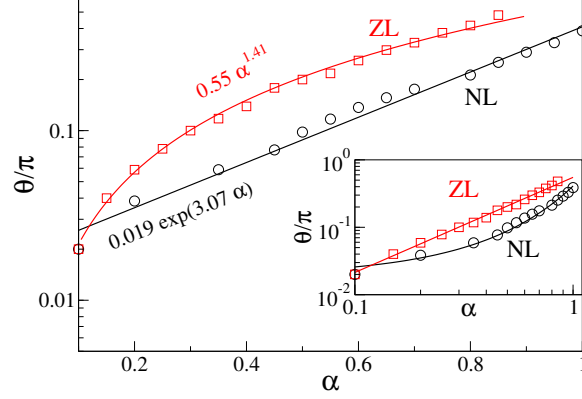


Figure 7: The pitch angle ( $\theta$ ) for different values of  $\alpha$  in both the NL and the ZL in log-linear scale (main figure) and in log-log scale (inset). The solid lines are the exponential fit (for NL) and the power law fit (for ZL). The actual fitted formulae are given on the plot near the curves.

chain is  $l$  for which the total angle change between  $i^{\text{th}}$  and  $i+l^{\text{th}}$  spin is  $2\pi$ . The length  $l$  is the wavelength of the incommensurate SDW. Therefore  $\theta$  can be defined as  $2\pi/l$ . The pitch angle  $\theta$  in the AF leg as a function of  $\alpha$  is plotted in Fig. 7 for the NL with black circle and for the ZL with red squares. The main figure shows the log-linear plot. The pitch angle for the NL follows exponential decay as shown in the main Fig. 7. The line represents the fitted curve with  $0.019 \exp(3.07\alpha)$ . The convention of symbols in the inset is the same as in the main figure. The inset of Fig. 7 shows the log-log plot of  $\theta/\pi$  vs.  $\alpha$ , which is fitted with  $0.55 \alpha^{1.41}$  for the ZL.

### 3.5. Large $\alpha$ limit

In the large  $\alpha > 1.14$  limit, the NL behaves as dimer of two nearest neighbor spins at different leg of ladder. The  $C(r)$  for  $\alpha = 1.15$  is very short ranged and is non-zero only for nearest neighbor spins as shown in Fig. 3(c). The GS energy is exactly equal to  $-\frac{3}{8}N\alpha$ . The AF 2-leg ladder has a short range order and has finite lowest energy gap (spin gap)  $\Delta = -3J_1/4$  in the perfect dimer limit. This energy is equivalent to breaking a singlet bond. The short range correlation in NL and gaped excitation are explained in the analytical Section 4.

In this limit the ZL system behaves as a single chain of  $N$  spins with nearest neighbor exchange interaction  $J_1$ . It is well known that the GS of spin-1/2 HAF chain is a spin fluid state and this phase can be characterized by the algebraic decay of spin-spin correlations and the gapless energy excitation. The transition point from the incommensurate SDW phase to the spin fluid in the ZL is at  $\alpha \approx 1.06$ .

## 4. Effective Hamiltonian for NL

In large inter-chain coupling limit the NL shows dimer phase as already mentioned in Section 3.5. To understand the dimer phase we treat the NL analytically in this section. Our aim is to find an effective Hamiltonian for the NL in the strong coupling limit i.e.,

for  $\alpha \gg 1$ . There is a very sharp critical  $\alpha$  for NL and the system has singlet GS for  $\alpha > \alpha_c$ .

In the strong rung coupling limit the system can be approximated as a collection of  $N/2$  rungs. The Hamiltonian then becomes  $H_{\text{rung}}^{\text{NL}}$  (see Eq. (2)). The GS of this Hamiltonian is  $2^{N/2}$  fold degenerate. Each of  $N/2$  rungs can be either in the state  $|S_0\rangle$  or  $|T_1\rangle$  with energies  $E(S_0) = -3J_1/4$  and  $E(T_1) = J_1/4$ .  $H_{\text{leg}}$  lifts the degeneracy and leads to an effective Hamiltonian that can be derived by standard many-body perturbation theory [49]. Following the same procedure mentioned in [50], we can write the spin operators in terms of the pseudo-spin-1/2 operators. Let us introduce pseudo spin-1/2 operators  $\tau_i$  to be acted on the states  $|S_0\rangle_i$  and  $|T_1\rangle_i$  of rung  $i$  following

$$\begin{aligned} \tau_i^z |S_0\rangle_i &= -\frac{1}{2} |S_0\rangle_i & \tau_i^z |T_1\rangle_i &= \frac{1}{2} |T_1\rangle_i \\ \tau_i^+ |S_0\rangle_i &= |T_1\rangle_i & \tau_i^+ |T_1\rangle_i &= 0 \\ \tau_i^- |S_0\rangle_i &= 0 & \tau_i^- |T_1\rangle_i &= |S_0\rangle_i \end{aligned} \quad (6)$$

One can express the original operators in Eq. (2) in terms of the pseudo-spin operators. This can be done by inspection and are given by:

$$\begin{aligned} S_{2i-1}^+ &= -\frac{1}{\sqrt{2}} \tau_i^+ & S_{2i+1}^+ &= \frac{1}{\sqrt{2}} \tau_i^+ \\ S_{2i-1}^- &= -\frac{1}{\sqrt{2}} \tau_i^- & S_{2i+1}^- &= \frac{1}{\sqrt{2}} \tau_i^- \\ S_{2i-1}^z &= \frac{1}{2} \left( \tau_i^z + \frac{1}{2} \right) & S_{2i+1}^z &= \frac{1}{2} \left( \tau_i^z + \frac{1}{2} \right) \end{aligned} \quad (7)$$

Substituting these expressions into the Hamiltonian we get the effective Hamiltonian as:

$$\begin{aligned} H &= H_0 + J_{xy}^{\text{eff}} \sum_{i=1}^{N/2} \frac{1}{2} (\tau_i^+ \tau_{i+1}^- + \tau_i^- \tau_{i+1}^+) \\ &\quad + J_z^{\text{eff}} \sum_{i=1}^{N/2} \tau_i^z \tau_{i+1}^z + h_{\text{eff}} \sum_{i=1}^{N/2} \tau_i^z + C_0 \end{aligned} \quad (8)$$

where  $J_{xy}^{\text{eff}} = \frac{J_1+J_2}{2}$ ,  $J_z^{\text{eff}} = \frac{J_1+J_2}{4}$ ,  $h_{\text{eff}} = \frac{J_1+J_2}{4}$ , and  $C_0 = \frac{J_1+J_2}{4}$ . For the AF-F ladder  $J_1 = -J_2 = J$ , therefore at strong coupling limit  $H = H_0$ . The critical rung interactions are given in the Appendix.

## 5. Discussion and Conclusions

In this paper We studied F-AF ladder models with an antiferromagnetic leg and a ferromagnetic leg coupled through antiferromagnetic rungs. Two types (NL and the ZL) of ladders are considered (see Fig. 1). It is clear from Figs. 1(a) and (b) that irrespective of the structure both NL and ZL are frustrated in nature. Our calculation suggests that both NL and ZL show incommensurate SDW phase for  $0 < \alpha < \alpha_c$  in the thermodynamic limit.

We show that the ZL exhibits some similarities with the NL in the low  $\alpha$  limit, but have remarkable differences in the large  $\alpha$  limit. In small and intermediate  $\alpha$  limit both ladders exhibit incommensurate SDWs. In large  $\alpha$  limit the ZL behaves like single HAF chain and the NL shows an exact dimer phase. The pitch angle in the incommensurate SDW phase of the ZL show algebraic variation, whereas it changes exponentially in the NL. The spin density fluctuation  $C^F(r)$  follows the power law in both legs for both type of ladders as shown in Fig. 4; this behavior is similar as partially magnetized HAF chain. Most of HAF ladder [7, 12] or frustrated ladder [21, 22, 51] shows exponential behavior of correlation function in the spiral phase. The critical value  $\alpha_c$  for incommensurate SDW to singlet dimer transition in NL is almost independent of system size, and can be explained by analytical calculation of perturbation theory of this system. The finite size effect on  $\alpha_c$  in ZL is also weak.

For  $\alpha < 0.9$  in both the ladders  $\langle M \rangle \propto \alpha^2$  as shown in Fig. 2.  $\langle M \rangle$  decreases rapidly to zero for  $\alpha > 0.9$ . Interestingly for both the ladders in  $\alpha < 0.9$  regime, the total spin density on the F leg  $\rho_T^F \propto \alpha^2$  whereas on the AF leg  $\rho_T^F \propto \alpha$  for  $\alpha < 0.9$  as shown in Fig. 6. The spin density  $\rho_T^{AF}$  at AF-leg of both the systems is always negative, and  $\rho_T^{AF}$  for the ZL have higher magnitude than the NL contrary to the  $\rho_T^F$ .

In the mean field limit this model can be approximated as a partially magnetized HAF chain, at least in small coupling limit. Here the F-leg act as a uniform external magnetic field on the AF-leg. Using the Heisenberg Hamiltonian with anisotropy constant, Suhl and Schuller explained the effective bias field  $H_{\text{eff}} \propto J_c^2$  in Eq. (12) of [24], where  $J_c$  is the exchange interaction strength between two layers. However as shown in Fig. 2,  $\langle M \rangle \propto \alpha^2$  in both the systems for  $\alpha < 0.9$ . Assuming the magnetization in these systems is proportional to field ( $h$ ), we obtain  $h \propto \alpha^2$ . T. M. Hong suggested in [25] that in low temperature limit  $h \propto J_c$ . Our calculation agrees very well with the calculations in [24]

In conclusion, we consider F-AF two-legged spin-1/2 ladders with antiferromagnetic rungs. In the finite  $\alpha < 1.0$  regime we notice the incommensurate SDW phase in both the ladders. We also notice that the NL behaves like a collection of independent dimers for  $\alpha > 1.14$ , whereas the ZL behaves like a single spin-1/2 chain for  $\alpha > 1.06$ . The magnetization on the F leg varies as  $J_1^2$ , whereas it varies linearly with  $J_1$  on AF leg.

## Acknowledgement

MK thanks DST for Ramanujan fellowship and computation facility provided under the DST project SNB/MK/14-15/137. We thank Z. G. Soos for his valuable comments.

## Appendix A. Critical rung interaction

According to the numerical analysis we find a sharp transition from the  $S_G > 0$  to  $S_G = 0$  at some critical value of  $\alpha$  for both the ladders. This critical value is independent of the system size. Let us consider a toy model of four spins as shown in Fig. 1(a). The eigenvalues in the  $S^z = 0$  sector are  $\frac{1}{4}(-2J_1 + J_2 + J_3)$ ,  $\frac{1}{4}(2J_1 + J_2 + J_3)$ ,  $-\frac{1}{4}\left(J_2 + J_3 + 2\sqrt{(J_2 - J_3)^2 + J_1^2}\right)$ ,  $-\frac{1}{4}\left(J_2 + J_3 - 2\sqrt{(J_2 - J_3)^2 + J_1^2}\right)$ ,  $-\frac{1}{4}\left(2J_1 + J_2 + J_3 + 2\sqrt{(-J_1 + J_2 + J_3)^2 + 3J_1^2}\right)$ ,

$-\frac{1}{4} \left( 2J_1 + J_2 + J_3 - 2\sqrt{(-J_1 + J_2 + J_3)^2 + 3J_1^2} \right)$  and the eigenvalues in the  $S^z = 1$  sector are  $\frac{1}{4}(-2J_1 + J_2 + J_3)$ ,  $\frac{1}{4}(2J_1 + J_2 + J_3)$ ,  $-\frac{1}{4} \left( J_2 + J_3 + 2\sqrt{(J_2 - J_3)^2 + J_1^2} \right)$ ,  $-\frac{1}{4} \left( J_2 + J_3 - 2\sqrt{(J_2 - J_3)^2 + J_1^2} \right)$ . The interactions are set to  $J_2 = -1$  and  $J_3 = 1$ , and  $J_1 = \alpha$  is a variable. This leads to the lowest two eigenvalues:  $E_0(S^z = 0) = -\frac{3}{2}\alpha$  and  $E_0(S^z = 1) = -\frac{1}{2}\sqrt{4 + \alpha^2}$ . As we consider the  $\alpha > 0$  case only, the critical value  $\alpha_c = \frac{1}{\sqrt{2}}$  for this toy model.

## References

## References

- [1] S. R. White, R. M. Noack, D. J. Scalapino, Resonating valence bond theory of coupled heisenberg chains, *Phys. Rev. Lett.* 73 (1994) 886–889. [doi:10.1103/PhysRevLett.73.886](#).
- [2] M. Kumar, A. Parvej, Z. G. Soos, Level crossing, spin structure factor and quantum phases of the frustrated spin-1/2 chain with first and second neighbor exchange, *J. Phys.: Condens. Matter* 27 (31) (2015) 316001. [doi:10.1088/0953-8984/27/31/316001](#).
- [3] T. Verkholyak, J. Streka, Quantum phase transitions in the exactly solved spin-1/2 heisenbergising ladder, *Journal of Physics A: Mathematical and Theoretical* 45 (30) (2012) 305001. [doi:10.1088/1751-8121/45/30/305001](#).
- [4] A. Honecker, F. Mila, M. Troyer, Magnetization plateaux and jumps in a class of frustrated ladders: A simple route to a complex behaviour, *The European Physical Journal B - Condensed Matter and Complex Systems* 15 (2) (2000) 227–233. [doi:10.1007/s100510051120](#).
- [5] A. W. Sandvik, E. Dagotto, D. J. Scalapino, Spin dynamics of  $\text{SrCu}_2\text{O}_3$  and the heisenberg ladder, *Phys. Rev. B* 53 (1996) R2934–R2937. [doi:10.1103/PhysRevB.53.R2934](#).
- [6] D. C. Johnston, J. W. Johnson, D. P. Goshorn, A. J. Jacobson, Magnetic susceptibility of  $(\text{vo})_2\text{p}_2\text{o}_7$ : A one-dimensional spin-1/2 heisenberg antiferromagnet with a ladder spin configuration and a singlet ground state, *Phys. Rev. B* 35 (1987) 219–222. [doi:10.1103/PhysRevB.35.219](#).
- [7] E. Dagotto, T. M. Rice, Surprises on the way from one- to two-dimensional quantum magnets: The ladder materials, *Science* 271 (5249) (1996) 618–623. [doi:10.1126/science.271.5249.618](#).
- [8] N. Maeshima, M. Hagiwara, Y. Narumi, K. Kindo, T. C. Kobayashi, K. Okunishi, [Magnetic properties of a  \$s = 1/2\$  zigzag spin chain compound  \$\(\text{n}2\text{h}5\)\text{cucl}\_3\$](#) , *Journal of Physics: Condensed Matter* 15 (21) (2003) 3607. URL <http://stacks.iop.org/0953-8984/15/i=21/a=309>
- [9] S. E. Dutton, M. Kumar, M. Mourigal, Z. G. Soos, J.-J. Wen, C. L. Broholm, N. H. Andersen, Q. Huang, M. Zbiri, R. Toft-Petersen, R. J. Cava, Quantum spin liquid in frustrated one-dimensional  $\text{licusbo}_4$ , *Phys. Rev. Lett.* 108 (2012) 187206. [doi:10.1103/PhysRevLett.108.187206](#).
- [10] M. Mourigal, M. Enderle, B. Fåk, R. K. Kremer, J. M. Law, A. Schneidewind, A. Hiess, A. Prokofiev, Evidence of a bond-nematic phase in  $\text{licuvo}_4$ , *Phys. Rev. Lett.* 109 (2012) 027203. [doi:10.1103/PhysRevLett.109.027203](#).
- [11] S.-L. Drechsler, O. Volkova, A. N. Vasiliev, N. Tristan, J. Richter, M. Schmitt, H. Rosner, J. Málek, R. Klingeler, A. A. Zvyagin, B. Büchner, Frustrated cuprate route from antiferromagnetic to ferromagnetic spin- $\frac{1}{2}$  heisenberg chains:  $\text{li}_2\text{zrcuo}_4$  as a missing link near the quantum critical point, *Phys. Rev. Lett.* 98 (2007) 077202. [doi:10.1103/PhysRevLett.98.077202](#).
- [12] E. Dagotto, J. Riera, D. Scalapino, Superconductivity in ladders and coupled planes, *Phys. Rev. B* 45 (1992) 5744–5747. [doi:10.1103/PhysRevB.45.5744](#).
- [13] K. Hijii, A. Kitazawa, K. Nomura, Phase diagram of  $S = \frac{1}{2}$  two-leg  $xxz$  spin-ladder systems, *Phys. Rev. B* 72 (2005) 014449. [doi:10.1103/PhysRevB.72.014449](#).
- [14] T. Vekua, G. I. Japaridze, H.-J. Mikeska, Phase diagrams of spin ladders with ferromagnetic legs, *Phys. Rev. B* 67 (2003) 064419. [doi:10.1103/PhysRevB.67.064419](#).
- [15] J. Almeida, M. A. Martin-Delgado, G. Sierra, Density-matrix renormalization group study of the bond-alternating  $s = 12$  heisenberg ladder with ferro-antiferromagnetic couplings, *Phys. Rev. B* 76 (2007) 184428. [doi:10.1103/PhysRevB.76.184428](#).
- [16] S. E. Dutton, M. Kumar, Z. G. Soos, C. L. Broholm, R. J. Cava, Dominant ferromagnetism in the spin-1/2 half-twist ladder 334 compounds,  $\text{ba}_3\text{cu}_3\text{in}_4\text{o}_{12}$  and  $\text{ba}_3\text{cu}_3\text{sc}_4\text{o}_{12}$ , *J. Phys.: Condens. Matter* 24 (16) (2012) 166001. [doi:10.1088/0953-8984/24/16/166001](#).

- [17] M. Kumar, S. E. Dutton, R. J. Cava, Z. G. Soos, Spin-flop and antiferromagnetic phases of the ferromagnetic half-twist ladder compounds  $\text{Ba}_3\text{Cu}_3\text{In}_4\text{O}_{12}$  and  $\text{Ba}_3\text{Cu}_3\text{Sc}_4\text{O}_{12}$ , J. Phys.: Condens. Matter 25 (13) (2013) 136004. [doi:10.1088/0953-8984/25/13/136004](#).
- [18] O. S. Volkova, I. S. Maslova, R. Klingeler, M. Abdel-Hafiez, Y. C. Arango, A. U. B. Wolter, V. Kataev, B. Büchner, A. N. Vasiliev, Orthogonal spin arrangement as possible ground state of three-dimensional shastry-sutherland network in  $\text{Ba}_3\text{Cu}_3\text{In}_4\text{O}_{12}$ , Phys. Rev. B 85 (2012) 104420. [doi:10.1103/PhysRevB.85.104420](#).
- [19] D. I. Badrtdinov, O. S. Volkova, A. A. Tsirlin, I. V. Solovyev, A. N. Vasiliev, V. V. Mazurenko, Hybridization and spin-orbit coupling effects in the quasi-one-dimensional spin- $\frac{1}{2}$  magnet  $\text{Ba}_3\text{Cu}_3\text{Sc}_4\text{O}_{12}$ , Phys. Rev. B 94 (2016) 054435. [doi:10.1103/PhysRevB.94.054435](#).
- [20] Z. G. Soos, A. Parvej, M. Kumar, Numerical study of incommensurate and decoupled phases of spin-1/2 chains with isotropic exchange  $j_1$ ,  $j_2$  between first and second neighbors, J. Phys.: Condens. Matter 28 (17) (2016) 175603. [doi:10.1088/0953-8984/28/17/175603](#).
- [21] M. Kumar, Z. G. Soos, Decoupled phase of frustrated spin- $\frac{1}{2}$  antiferromagnetic chains with and without long-range order in the ground state, Phys. Rev. B 88 (2013) 134412. [doi:10.1103/PhysRevB.88.134412](#).
- [22] R. Chitra, S. Pati, H. R. Krishnamurthy, D. Sen, S. Ramasesha, Density-matrix renormalization-group studies of the spin-1/2 heisenberg system with dimerization and frustration, Phys. Rev. B 52 (1995) 6581–6587. [doi:10.1103/PhysRevB.52.6581](#).
- [23] C. K. Majumdar, D. K. Ghosh, On nextnearestneighbor interaction in linear chain. ii, J. Math. Phys. 10 (8) (1969) 1399–1402. [doi:10.1063/1.1664979](#).
- [24] H. Suhl, I. K. Schuller, Spin-wave theory of exchange-induced anisotropy, Phys. Rev. B 58 (1998) 258–264. [doi:10.1103/PhysRevB.58.258](#).
- [25] T. M. Hong, Simple mechanism for a positive exchange bias, Phys. Rev. B 58 (1998) 97–100. [doi:10.1103/PhysRevB.58.97](#).
- [26] W. H. Meiklejohn, C. P. Bean, New magnetic anisotropy, Phys. Rev. 102 (1956) 1413–1414. [doi:10.1103/PhysRev.102.1413](#).
- [27] W. H. Meiklejohn, C. P. Bean, New magnetic anisotropy, Phys. Rev. 105 (1957) 904–913. [doi:10.1103/PhysRev.105.904](#).
- [28] J. Nogus, I. K. Schuller, Exchange bias, J. Magn. Magn. Mater. 192 (2) (1999) 203 – 232. [doi:10.1016/S0304-8853\(98\)00266-2](#).
- [29] M. Kiwi, Exchange bias theory, J. Magn. Magn. Mater. 234 (3) (2001) 584 – 595. [doi:10.1016/S0304-8853\(01\)00421-8](#).
- [30] A. Berkowitz, K. Takano, Exchange anisotropy – a review, J. Magn. Magn. Mater. 200 (13) (1999) 552 – 570. [doi:10.1016/S0304-8853\(99\)00453-9](#).
- [31] M. Finazzi, Interface coupling in a ferromagnet/antiferromagnet bilayer, Phys. Rev. B 69 (2004) 064405. [doi:10.1103/PhysRevB.69.064405](#).
- [32] A. P. Malozemoff, Random-field model of exchange anisotropy at rough ferromagnetic-antiferromagnetic interfaces, Phys. Rev. B 35 (1987) 3679–3682. [doi:10.1103/PhysRevB.35.3679](#).
- [33] N. C. Koon, Calculations of exchange bias in thin films with ferromagnetic/antiferromagnetic interfaces, Phys. Rev. Lett. 78 (1997) 4865–4868. [doi:10.1103/PhysRevLett.78.4865](#).
- [34] T. C. Schulthess, W. H. Butler, Consequences of spin-flop coupling in exchange biased films, Phys. Rev. Lett. 81 (1998) 4516–4519. [doi:10.1103/PhysRevLett.81.4516](#).
- [35] T. C. Schulthess, W. H. Butler, Coupling mechanisms in exchange biased films (invited), J. Appl. Phys. 85 (8) (1999) 5510–5515. [doi:10.1063/1.369878](#).
- [36] J.-V. Kim, R. L. Stamps, Defect-modified exchange bias, Applied Physics Letters 79 (17) (2001) 2785–2787. [doi:10.1063/1.1413731](#).
- [37] U. Nowak, A. Misra, K. D. Usadel, Domain state model for exchange bias, J. Appl. Phys. 89 (11) (2001) 7269–7271. [doi:10.1063/1.1358829](#).
- [38] Y. Sakurai, H. Kitatani, T. Ishiguro, Y. Ichinose, N. S. Kazama, Monte carlo approach for f-af coupling layers, IEEE Trans. Magn. 29 (1993) 3879.
- [39] D. Mauri, H. C. Siegmann, P. S. Bagus, E. Kay, Simple model for thin ferromagnetic films exchange coupled to an antiferromagnetic substrate, J. Appl. Phys. 62 (7) (1987) 3047–3049. [doi:10.1063/1.339367](#).
- [40] H. Xi, R. M. White, S. M. Rezende, Irreversible and reversible measurements of exchange anisotropy, Phys. Rev. B 60 (1999) 14837–14840. [doi:10.1103/PhysRevB.60.14837](#).
- [41] H. Xi, R. M. White, A theoretical study of interfacial spin flop in exchange-coupled bilayers, IEEE Trans. Magn. 36 (2000) 2635.
- [42] J. Geshev, Analytical solutions for exchange bias and coercivity in ferromagnetic/antiferromagnetic

- bilayers, Phys. Rev. B 62 (2000) 5627–5633. [doi:10.1103/PhysRevB.62.5627](#).
- [43] T. C. Schulthess, W. H. Butler, First-principles exchange interactions between ferromagnetic and antiferromagnetic films: Co on NiMn, a case study, J. Appl. Phys. 83 (11) (1998) 7225–7227. [doi:10.1063/1.367824](#).
  - [44] S. R. White, Density matrix formulation for quantum renormalization groups, Phys. Rev. Lett. 69 (1992) 2863–2866. [doi:10.1103/PhysRevLett.69.2863](#).
  - [45] K. A. Hallberg, New trends in density matrix renormalization, Advances in Physics 55 (5-6) (2006) 477–526.
  - [46] U. Schollwöck, The density-matrix renormalization group, Rev. Mod. Phys. 77 (2005) 259–315.
  - [47] M. Kumar, Z. G. Soos, D. Sen, S. Ramasesha, Modified density matrix renormalization group algorithm for the zigzag spin- $\frac{1}{2}$  chain with frustrated antiferromagnetic exchange: Comparison with field theory at large  $J_2/J_1$ , Phys. Rev. B 81 (2010) 104406. [doi:10.1103/PhysRevB.81.104406](#).
  - [48] D. Dey, D. Maiti, M. Kumar, An efficient density matrix renormalization group algorithm for chains with periodic boundary condition, Papers in Physics 8 (2016) 080006.
  - [49] P. Fulde, Electron Correlations in Molecules and Solids, 3rd Edition, Springer-Verlag, 1995.
  - [50] F. Mila, Ladders in a magnetic field: a strong coupling approach, Eur. Phys. J. B 6 (2) (1998) 201–205. [doi:10.1007/s100510050542](#).
  - [51] S. R. White, I. Affleck, Dimerization and incommensurate spiral spin correlations in the zigzag spin chain: Analogies to the kondo lattice, Phys. Rev. B 54 (1996) 9862–9869. [doi:10.1103/PhysRevB.54.9862](#).